An Area-Integrating Volume Velocity Transducer for Vibroacoustic Reciprocity Applications in Vehicles

K.R. Holland and F.J. Fahy

ISVR Technical Report No 266

February 1997

SCIENTIFIC PUBLICATIONS BY THE ISVR

Technical Reports are published to promote timely dissemination of research results by ISVR personnel. This medium permits more detailed presentation than is usually acceptable for scientific journals. Responsibility for both the content and any opinions expressed rests entirely with the author(s).

Technical Memoranda are produced to enable the early or preliminary release of information by ISVR personnel where such release is deemed to the appropriate. Information contained in these memoranda may be incomplete, or form part of a continuing programme; this should be borne in mind when using or quoting from these documents.

Contract Reports are produced to record the results of scientific work carried out for sponsors, under contract. The ISVR treats these reports as confidential to sponsors and does not make them available for general circulation. Individual sponsors may, however, authorize subsequent release of the material.

UNIVERSITY OF SOUTHAMPTON

INSTITUTE OF SOUND AND VIBRATION RESEARCH

FLUID DYNAMICS AND ACOUSTICS GROUP

An Area-Integrating Volume Velocity Transducer for Vibroacoustic Reciprocity Applications in Vehicles

by

K R Holland and F J Fahy

ISVR Technical Report No. 266

February 1997

Approved: Group Chairman, P A Nelson
Professor of Acoustics

CONTENTS

LIST OF ILLUSTRATIONS

LIST OF SYMBOLS

A area (m^2)

G cross-spectrum

H Green function

$\boldsymbol{r}$ position in enclosed volume

S_p spectrum of mean-squared pressure

N number of elements

v signal voltage (V)

ω radial frequency (radians/s)

1 Principle of The Vibroacoustic Reciprocity Method as Applied to Sound Radiation from Vibrating Surfaces

1.1 Basic Theory

The spectrum of the mean squared pressure at a point (r) in an enclosed volume generated by vibration of the enclosure surfaces is given by

$$S_{pr}(\omega) = \iint\limits_{A_i A_j} G(v_i, v_j, \omega) \, H_{ir}^*(\omega) H_{jr}(\omega) \, dA_i \, dA_j \ , \tag{1}$$

where i and j represent points on the enclosure surface, G is the cross-spectrum of surface normal velocities at points i and j, and H_{ir} and H_{jr} are the complex transfer functions (Green functions) between unit volume velocities of the surface at points i and j and the sound pressure at point r.

If the surface is subdivided into N finite elemental areas ΔA, equation (1) may be approximated by

$$S_{pr}(\omega) \approx \sum_i^N \sum_j^N G(q_i, q_j, \omega) \, H_{ir}^*(\omega) H_{jr}(\omega) \ , \tag{2}$$

where G is now the cross-spectrum of elemental volume velocities of surface elements ΔA_i and ΔA_j, and H refers to the centre points of the surface elements. The cross-terms corresponding to $i = j$ represent the effect of interference between sound radiated by different surface elements.

The mean square pressure in a frequency band $\Delta\omega = \omega_2 - \omega_1$ may be obtained from equation (2) by integration over the frequency band.

In cases where the acoustic damping of the enclosed volume is sufficiently high, distinct acoustic modal resonances are not observed, and the phase of the cross-spectrum varies much more rapidly with frequency than the phases of the transfer functions H. Under these circumstances, it may be acceptable to take the frequency-average values of the transfer functions outside the integral in equation (2). The remaining frequency integral of G is equal to the zero-time-delay cross-correlation function of the surface volume velocity, which is known to decay with separation distance between points i and j, especially when many modes of the vibrating surface have resonance frequencies within the chosen frequency band, and where a number of uncorrelated sources of vibration act simultaneously.

The vibroacoustic transfer functions H may be determined by a reciprocal technique, in which an omni-directional sound source is placed at the target point of interest (e.g. vehicle occupant's head) and the transfer function between the source volume velocity and the resulting blocked pressure at the centre of each surface element is evaluated.

1.2 Practical Considerations

The maximum acceptable size of the discrete surface elements may also be determined from reciprocity considerations. With an omni-directional sound source placed at the target point, the spatial rate of change of the magnitude and phase of the resulting sound pressure field in the blocked (rigid) surface of the enclosure indicates the degree of spatial resolution required.

The vibrational field of the surface of a typical vehicle enclosure will exhibit a wide range of spatial frequencies (wavenumber components), of which only those matching rather closely those of the reciprocally induced blocked pressure field generate significant pressure components at the target point. The largest significant surface wavenumber will be close to the acoustic wavenumber at the frequency considered: most of the significant components will be far smaller because of the geometry of the system. Point measurements of surface velocity (for example, by means of an accelerometer) do not discriminate between high (unimportant) and low (important) surface wavenumbers, and hence can produce serious bias errors if used to estimate $G(q_i, q_j, \omega)$ in equation (2). This phenomenon is illustrated by Figures 1 and 2 which show theoretical and measured examples respectively of the overestimation of the sound radiated from a plate when point velocity measurements are considered.

1.3 Function of the Volume Velocity Transducer

The function of the non-contact volume velocity transducer is to act as a low-pass surface wavenumber filter, thereby suppressing the source of bias error. Figures 3 and 4 are equivalent to figures 1 and 2 with the point velocities replaced by area-integrated velocities. The improvement in estimation of the radiated sound is clear. The obviation of the need to attach a vibration transducer to the vibrating surface also facilitates measurements on non-solid surfaces (e.g. soft trim) and allows spatial averaging to be performed by means of scanning over surface elements larger than the entire area of the transducer, which speeds up the measurement process at low frequencies, for which larger discrete elements are acceptable.

Figure 1   Theoretical Estimation of the Sound Radiated by a Baffled Rectangular Plate to a Far-Field Point using Point Sampling of the Velocity Field.
- - - Analytic Result, —— Point-Sample Estimate

Figure 2 Measured Estimation of the Sound Radiated by a Rectangular Plate to a Point in a Reverberant Room using Point Sampling of the Velocity Field.
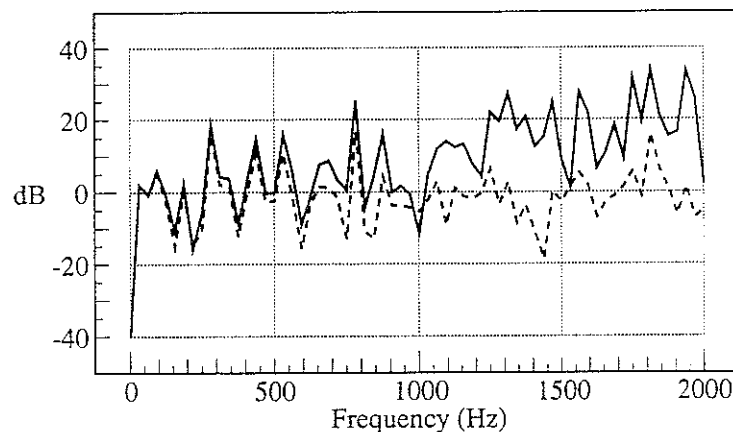

Figure 3 Theoretical Estimation of the Sound Radiated by a Baffled Rectangular Plate to a Far-Field Point using Area Integrated Sampling of the Velocity Field.
- - - Analytic Result, —— Area Integrated Sample Estimate
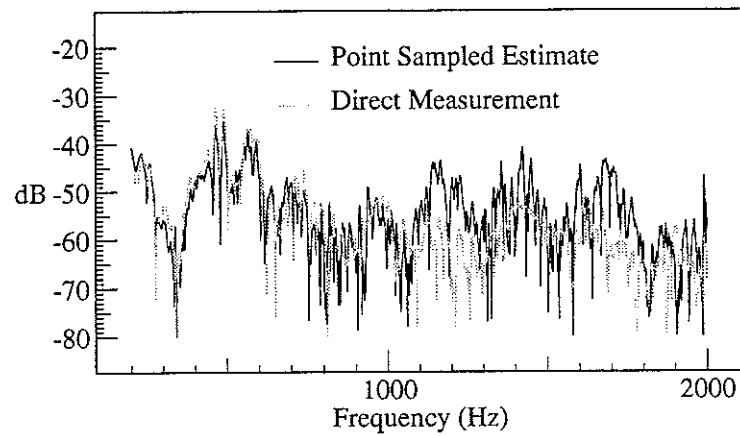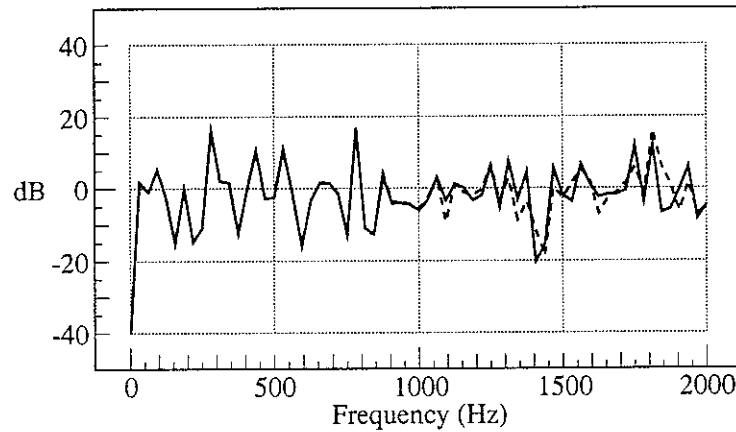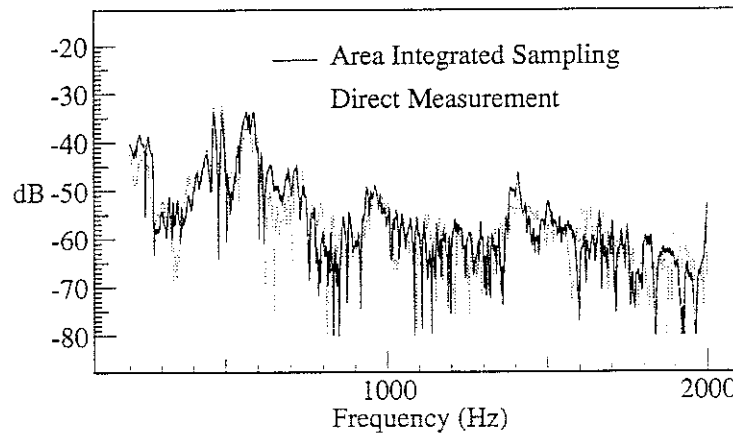

Figure 4 Measured Estimation of the Sound Radiated by a Rectangular Plate to a Point in a Reverberant Room using Area Integrated Sampling of the Velocity Field.

1.4 The Problem of Non-Coherent Surface Volume Velocities

In cases where the enclosure field is generated by a single input, where all elemental volume velocities are fully coherent, the determination of the cross-spectrum of elemental volume velocities requires only one transducer, and only one measurement per element; the cross-spectra may then be replaced by transfer functions between the transducer output and a suitable phase reference signal, thus:

$$S_{pr}(\omega) = |v_{ref}(\omega)|^2 \left| \sum_i^N \frac{v_i(\omega)}{v_{ref}(\omega)} A_i H_{ir} \right|^2 , \tag{3}$$

where v_{ref} is the phase reference signal. The in-car validation test (section 5) has been made under this condition.

However, when the enclosure is excited by multiple independent sources, the volume velocities are not fully coherent. In this case, the complete matrix of elemental volume velocity cross-spectra is required, which requires an enormous measurement effort. This problem has not been addressed in the present test programme which has been aimed at validating the transducer and basic measurement technique. However, the availability of the volume velocity transducer, used in matched pairs, will enable the statistical characteristics of the surface volume velocity distribution of operating vehicles to be studied. It is possible that the failure of deterministic models of vehicle vibration response to represent these statistical characteristics constitutes a major cause of predictive uncertainty.

2 The ISVR Volume Velocity Transducer

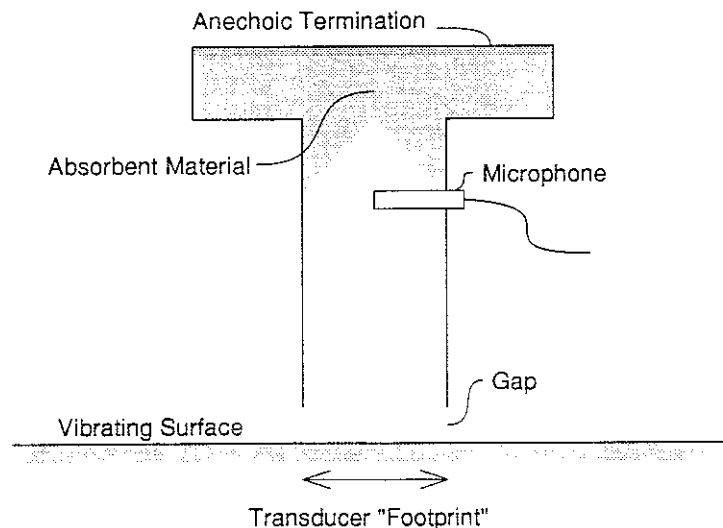The principle of the transducer is illustrated by Figure 5.

Figure 5 Principle of the Transducer

A uniform tube containing a small electret microphone is closed by an almost anechoic termination. With the mouth of the transducer tube close to a vibrating surface, a plane wave is

generated by the motion of the surface covered by the mouth of the tube. The contribution from the vibrating surface outside this area is relatively small provided that the distance of the mouth plane from this surface is less than about 20% of the mouth width. The ingress of sound from the surrounding volume is generally unimportant unless the level of vibration of the surface under the mouth is very low. If this condition is suspected to exist, a simple check can be made: the mouth of the tube is lowered toward the surface and the microphone response is monitored. If the influence of the external field is dominant, it will progressively decrease as the stand-off distance is decreased: on the other hand, the contribution from the surface will change very little.

The transducer can be calibrated by means of a reciprocity technique (see [1 & 2]). The microphone is replaced by a small omni-directional sound source. The mouth of the tube is placed firmly against a plane rigid surface into which the same microphone is set, and the transfer function between the input to the source and the microphone signal is determined. Then the mouth of the tube is placed at its normal stand-off distance, and the space-average transfer function is determined by scanning the tube mouth over the microphone position. The ratio of the two transfer functions so determined is independent of the source strength, and yields the transducer calibration.

The correct operation of the tube may be checked by means of comparison between its output when placed in position above a thin vibrating plate and an estimate of volume velocity determined from a large number of miniature accelerometer measurements made on a grid of points in the plate. This test is severe, because the vibration field of a thin plate contains a wide range of wavenumber components and is very non-uniform.

Although the presence of the anechoic termination is not strictly essential for the operation of the transducer, it does give rise to a calibration curve which is a smooth function of frequency and reduces the sensitivity of this calibration to the distance between the tube end and the surface being measured. The anechoic termination also allows the transducer to be calibrated using the reciprocal technique described above. A space-efficient anechoic termination has been proposed by Dalmont et al [3], which consists of a rapid cross-section expansion terminated by a resistive layer matched to the area ratio of the expansion. In its basic form the termination is only effective at low frequencies, but performance is extended to higher frequencies if sound absorbing treatments are applied to the cavity between the expansion and the resistive layer.

The length of the tube between the open mouth and the microphone is chosen by considering the rate of decay of higher order (non plane wave) modes within the frequency of interest. This length can be minimised by careful choice of the position of the microphone across the tube section. An axially mounted microphone was chosen as offering the best attenuation without the additional complication of using more than one microphone. Figure 6 shows some photographs of the prototype transducer.
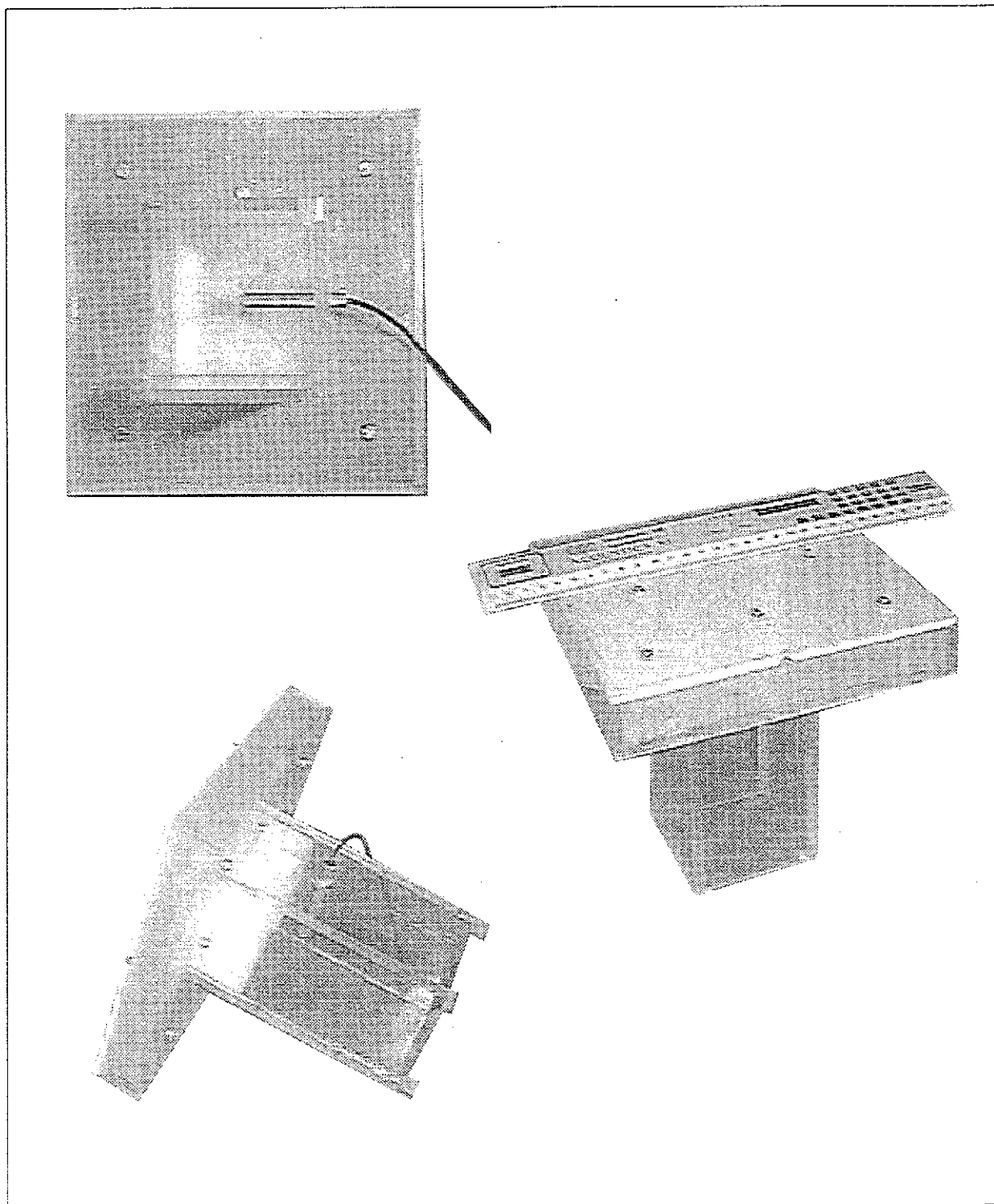
Figure 6 The Prototype Transducer.

3 Calibration of the Transducer

3.1 Spatial Selectivity.

The reciprocal calibration procedure (section 2) provides a means for investigating the spatial selectivity of the transducer. Figure 7 shows a grid of microphone position points relative to the transducer footprint. Figure 8 shows the sound level at the microphone positions relative to that on the transducer axis at 400Hz and 1600Hz. Figure 9 shows the 'overlap' selectivity that would result from the measurement of adjacent surface elements.
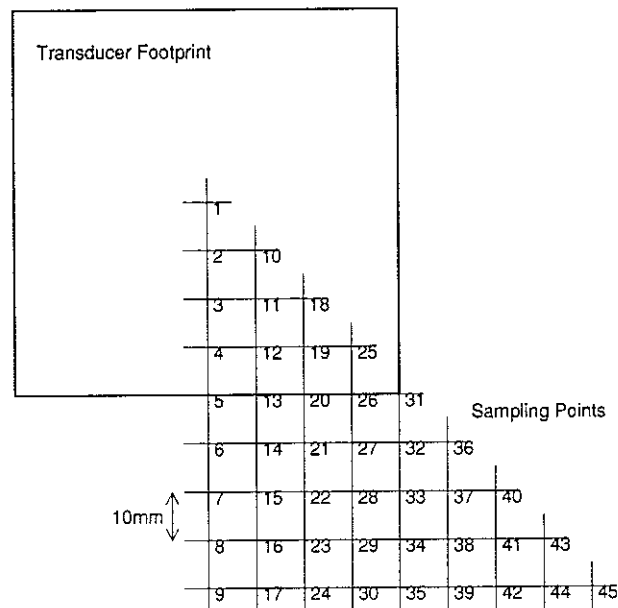
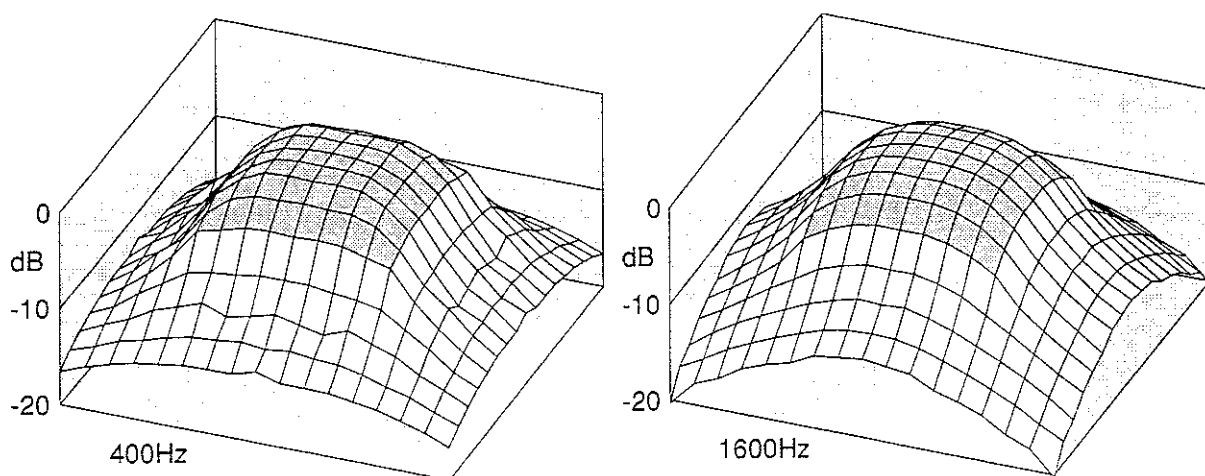*Figure 7 Map of Spatial Selectivity Microphone Positions*

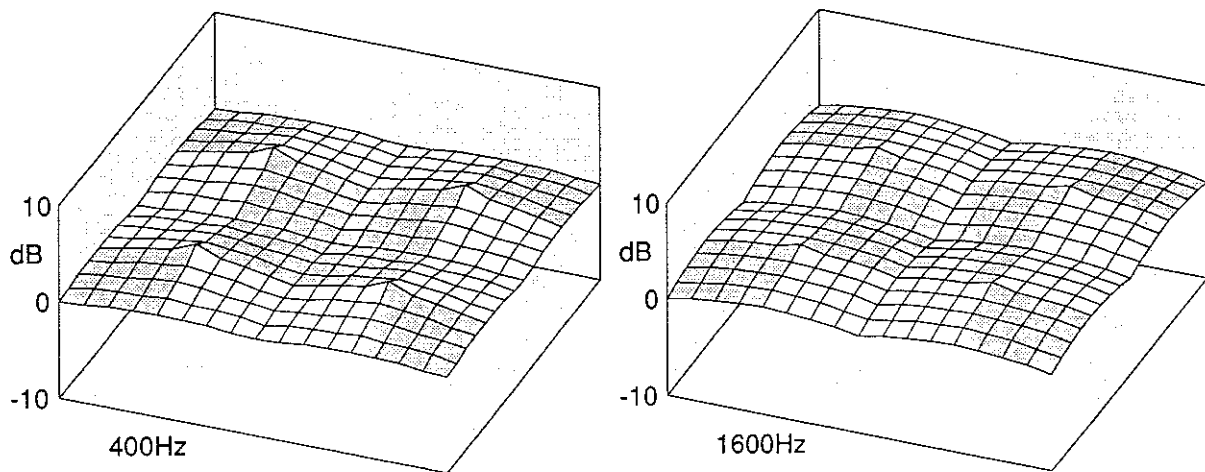*Figure 8 Spatial Selectivity for Transducer*

Figure 9 Spatial Overlap Selectivity for Transducer

3.2 Area-Integrated Calibration.

One of the main advantages of the transducer over conventional vibration measurement devices, is its ability to integrate the velocity of the surface beneath the tube end. The spatial selectivity results show that the sensitivity of the transducer is lower at the edge of this area than at the centre; it follows therefore that the sensitivity of the transducer to a distribution of velocity will be lower than that to a point monopole on axis. Figure 10 shows a comparison between the calibration curve for a point monopole on a surface and an area-integrated calibration, achieved by sweeping the tube end over the microphone whilst the measurement was taken. The results show a frequency independent reduction in sensitivity of 2dB for the area averaged calibration compared to the axial monopole calibration. This result is in accordance with integration of the spatial sensitivity results.
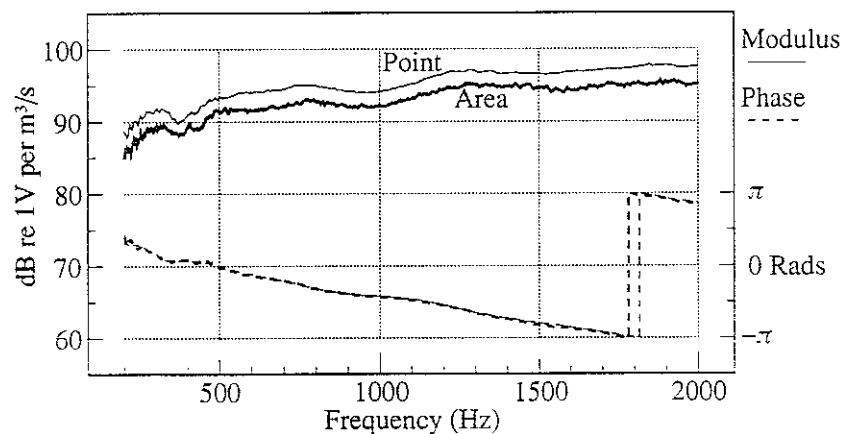

Figure 10 Comparison between Point Monopole and Area-Integrated Calibration Curves

3.3 Hand-Held Operation.

In real measurement situations, the transducer is likely to be hand-held during operation. It is unlikely that an operator would be capable of holding the transducer absolutely still during a measurement, so some variation in the size of the gap and the position of the tube-end is inevitable. Figure 11 shows five consecutive measurements of the volume velocity of part of a thin plate taken using the transducer. The transducer was hand-held during the measurements and no special effort was expended by the operator to maintain the position of the tube-end. The results show an encouraging lack of sensitivity to precise positioning of the transducer.
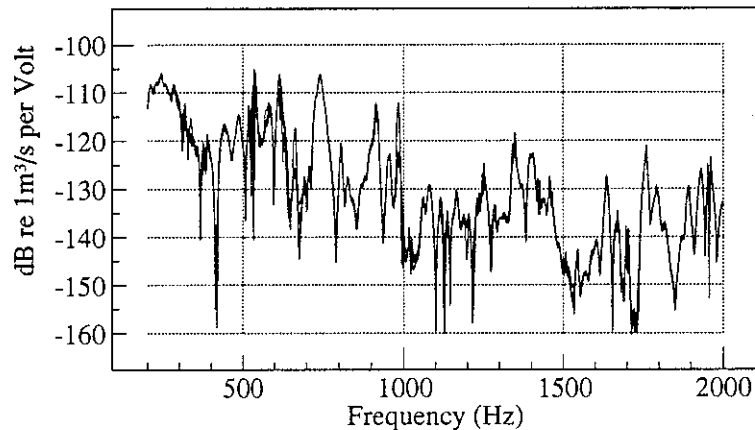

Figure 11   Repeatability of Hand-Held Measurement (5 times)

3.4 Multi-Accelerometer Check.

An estimate of the volume velocity of part of a vibrating surface may be found by measuring the velocity at a large number of points over the area using an accelerometer and summing all of the measurements together. Figure 12 shows a comparison between a measurement of the volume velocity of part of a thin vibrating plate using the transducer and that estimated from 49 accelerometer positions. The difference between the two curves cannot be attributed to errors in the transducer measurement only as the accelerometer measurements are influenced by discretisation of the surface and by the finite mass (0.7g) of the accelerometer.
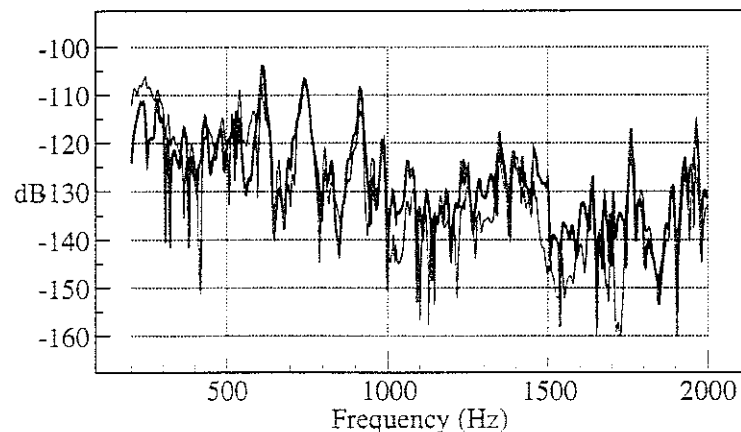

Figure 12   Comparison between transducer measurement (thin line) and 49 accelerometer positions (thick line)

4 The In-Car Validation Test

4.1 Description of Validation Test.

Figure 13 shows the vehicle that was selected for the validation test and figures 14, 15, 16 and 17 shows views of the inside of the cab. The seats and steering wheel have been removed and all apertures including the foot wells have been covered with stiff card and sealed with heavy adhesive tape and modelling clay. The figures show the entire interior surface of the cab marked off by means of tape into 1604 elements measuring 75mm × 75mm to match the transducer footprint. Excitation of the vehicle was via a loudspeaker placed under the cab close to the front of the engine. The surface normal volume velocity of the interior of the cab was mapped by measuring the transfer function between the transducer microphone signal and that of a reference microphone mounted close to the loudspeaker, for each element in turn. Figures 18 to 21 show the distribution of velocity over the surface of the cab at frequencies of 400Hz, 600Hz, 1000Hz and 1600Hz respectively.

The Green functions relating the velocity of an element to the sound pressure at a point in the cab were measured reciprocally by mounting a calibrated monopole source at the point of interest and measuring the pressure on each element in turn using a miniature microphone attached to the surface using adhesive tape. To avoid structural excitation of the cab, the source was suspended from the roof via three wires. All of the surfaces within the cab were assumed to contribute to the interior noise with the exception of the roof – the trim of which was assumed to act as a passive absorber. Figures 22 to 25 show the distribution of Green functions over the surface of the cab at frequencies of 400Hz, 600Hz, 1000Hz and 1600Hz respectively.

The contribution of each of the elements to the overall noise level at the interior point can be estimated by multiplying each of the measured velocity transfer functions with the associated Green function. Figures 26 to 29 show the distribution over the surface of the cab of the contribution to the noise level at frequencies of 400Hz, 600Hz, 1000Hz and 1600Hz respectively.

The validity of the technique can only be checked by comparing the noise level predicted by summing over the contribution of all the elements (eq. (3)) with a directly measured noise level. The direct measurement was achieved by mounting a microphone in a plate placed over the radiation aperture of the monopole source (suspended at the interior point) and measuring the transfer function between the output from this microphone and the reference microphone close to the excitation loudspeaker. Clearly this comparison relies on the interior noise being generated by vibration of the interior surfaces of the cab alone; it was for this reason that the entire interior surface had to be measured (except the passive roof) and that all possible apertures were sealed.

Initial tests highlighted a problem that occurred when measuring elements having very low volume velocity. The reverberant sound level within the vehicle cab gave rise to a higher signal at the transducer microphone than that due to the surface vibration. This problem was alleviated by closing the gap between the open tube end and the surface with a 'skirt' of lightweight plastic foam. The mechanical impedance of the skirt is sufficiently low that it has negligible effect on the vibration of the surface (the contact pressure is very low) and radiates negligible sound from its own vibration. An additional bonus from the use of the skirt is that the calibration curve is

now a smoother function of frequency, and the point monopole and area averaged calibrations are now similar. Figure 30 shows the calibration curve for the transducer with the skirt fitted; this can be compared with figure 10. The vibration of those elements that are physically inaccessible to the transducer were measured with a miniature accelerometer placed at the centre of the element. All measurements were taken using a portable dual-channel FFT analyser (Diagnostic Instruments type PL202) set to 1600 points on a baseband of 2kHz, and the excitation signal was white noise. The coherence function was monitored in real time during all of the measurements to alert the experimenter to any instances of poor signal-to-noise ratio or changes in conditions such as mechanical impact on the transducer.
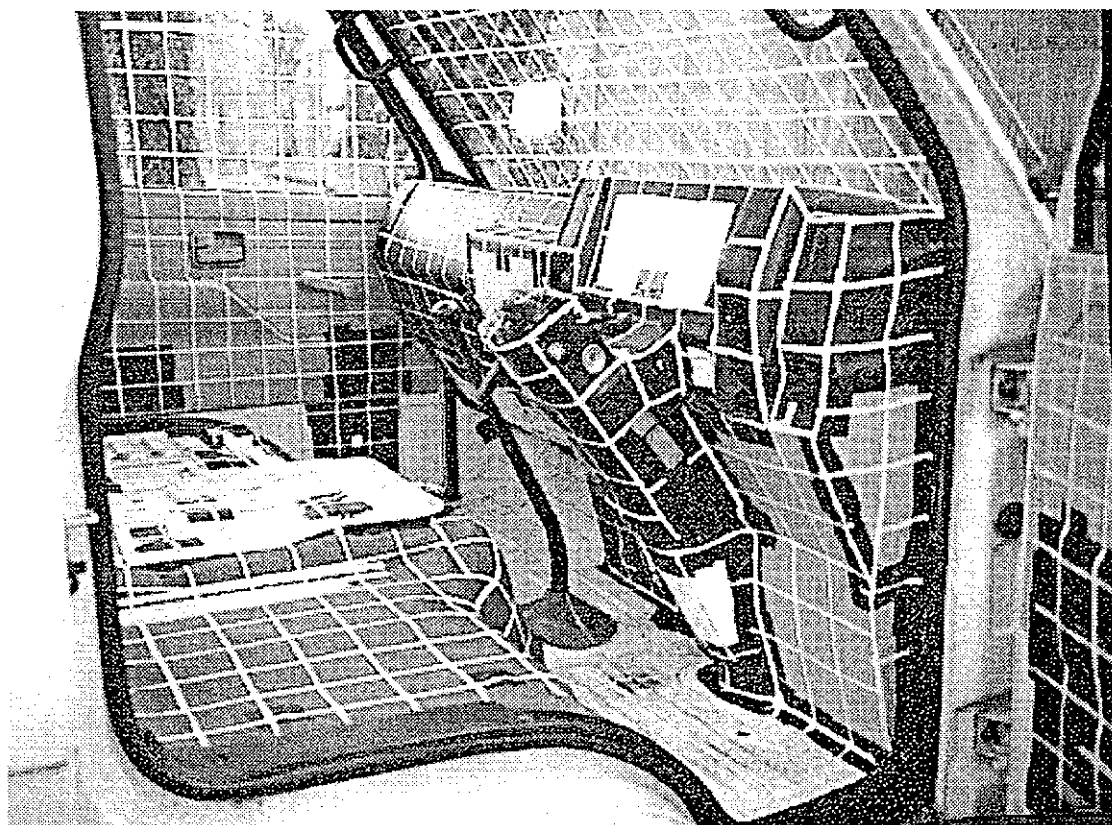

Figure 13 The Vehicle used in the Validation Test

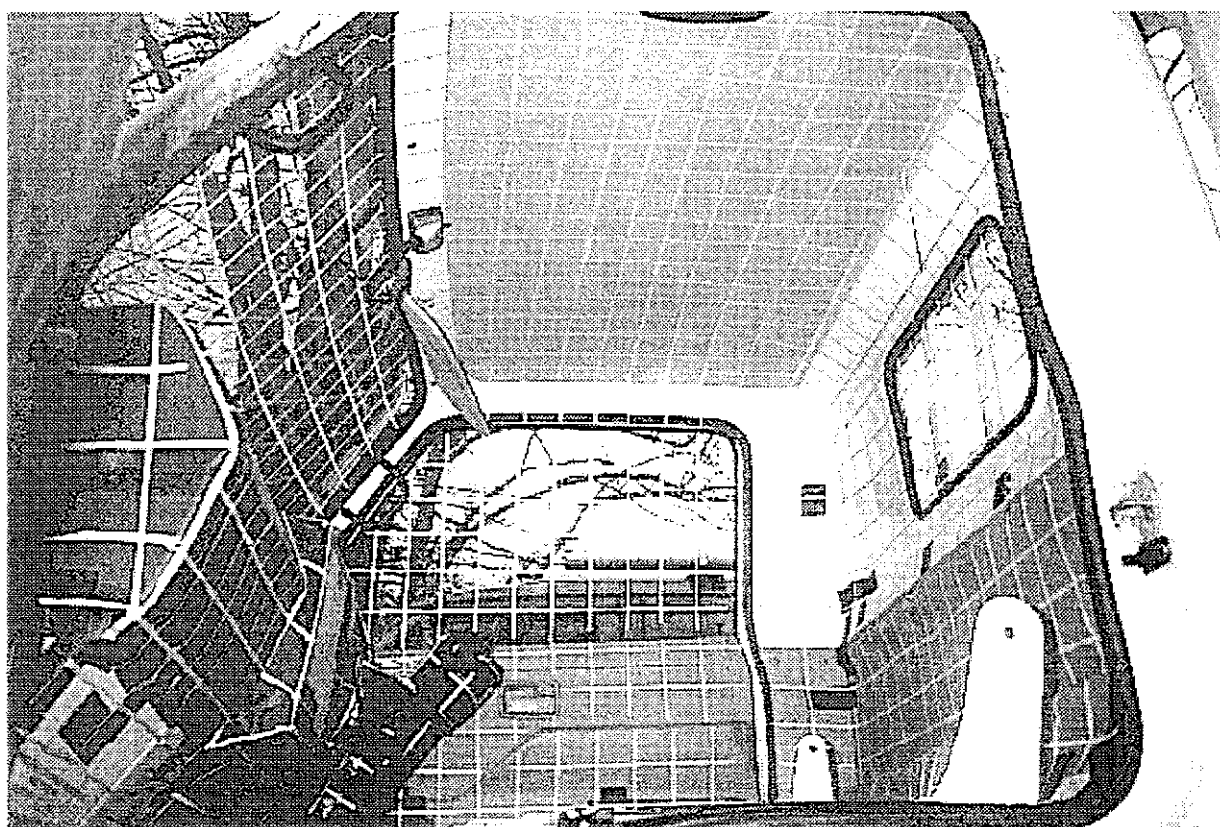*Figure 14 The Inside of the Vehicle showing Division into Elements*

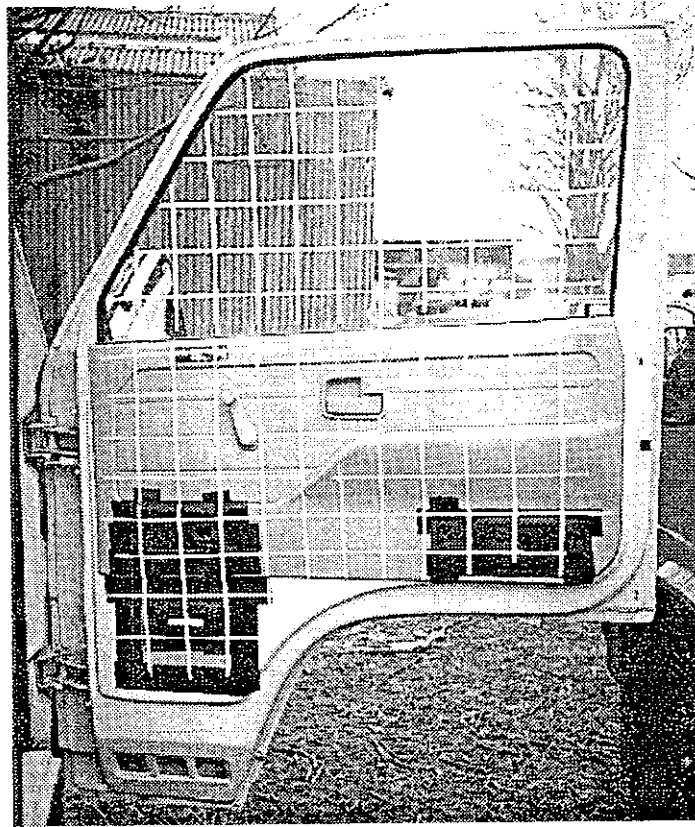*Figure 15 The Inside of the Vehicle showing Division into Elements*

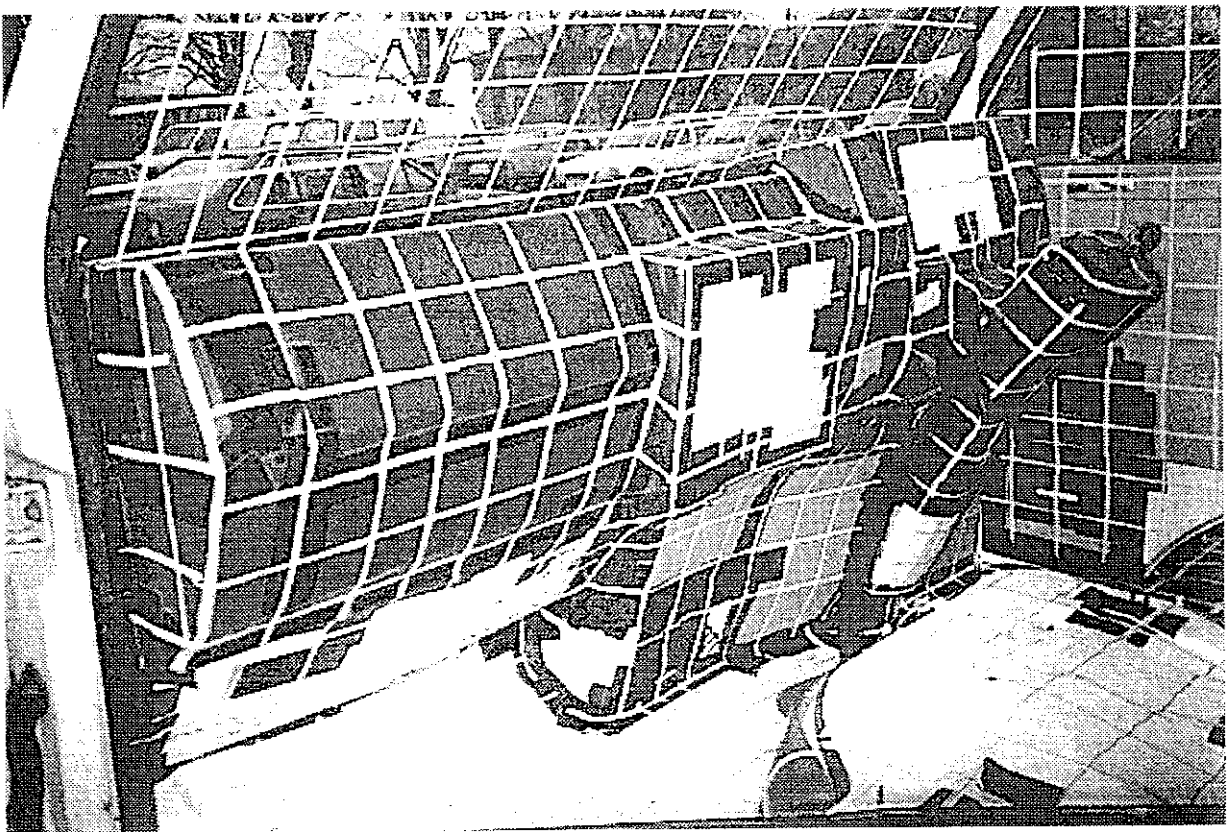*Figure 16 The Door of the Vehicle showing Division into Elements*

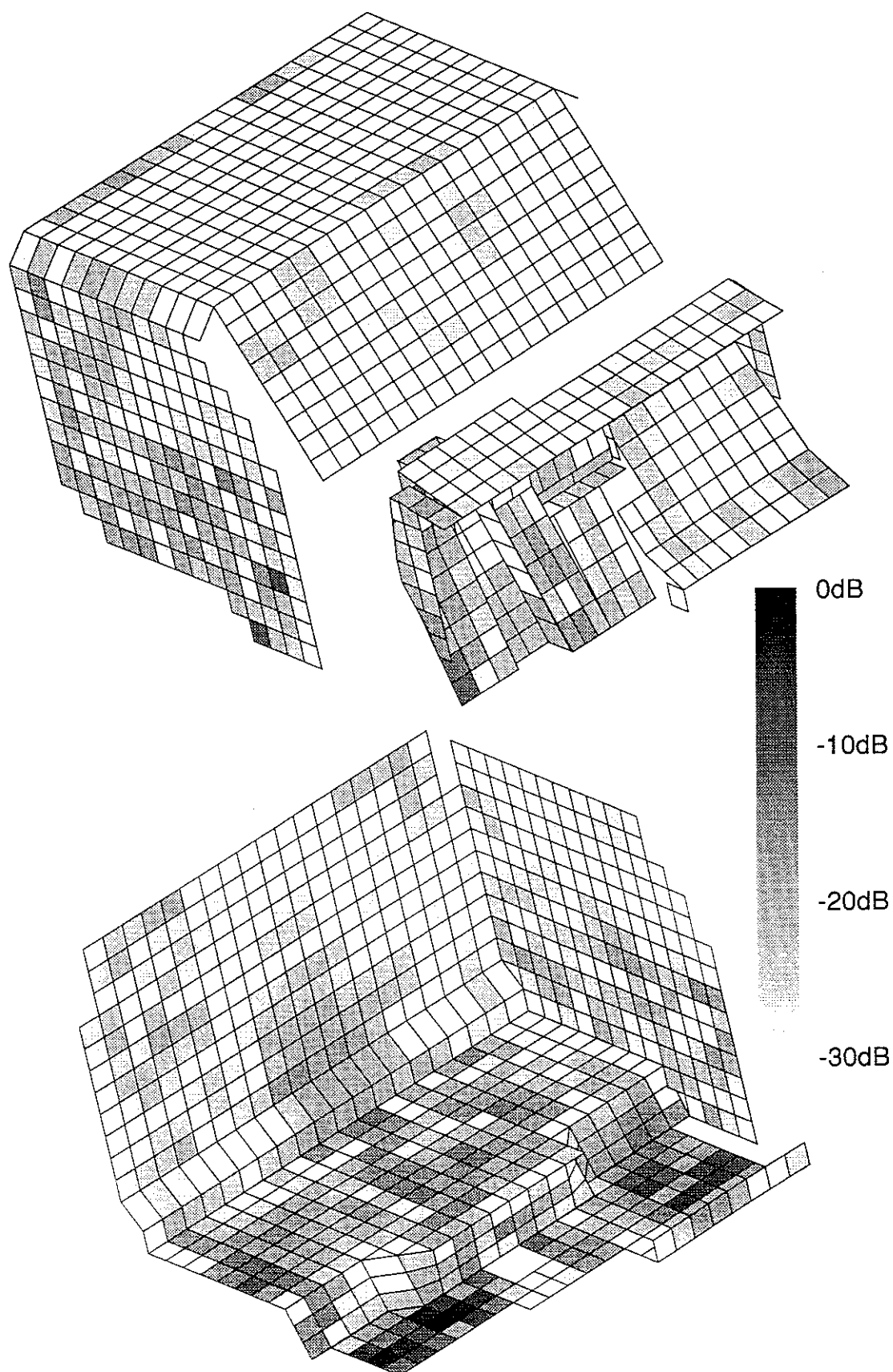*Figure 17 The ... Division into Elements*

Figure 18 Distribution of Volume Velocity over the Interior Surface of the Vehicle Cab at 400Hz
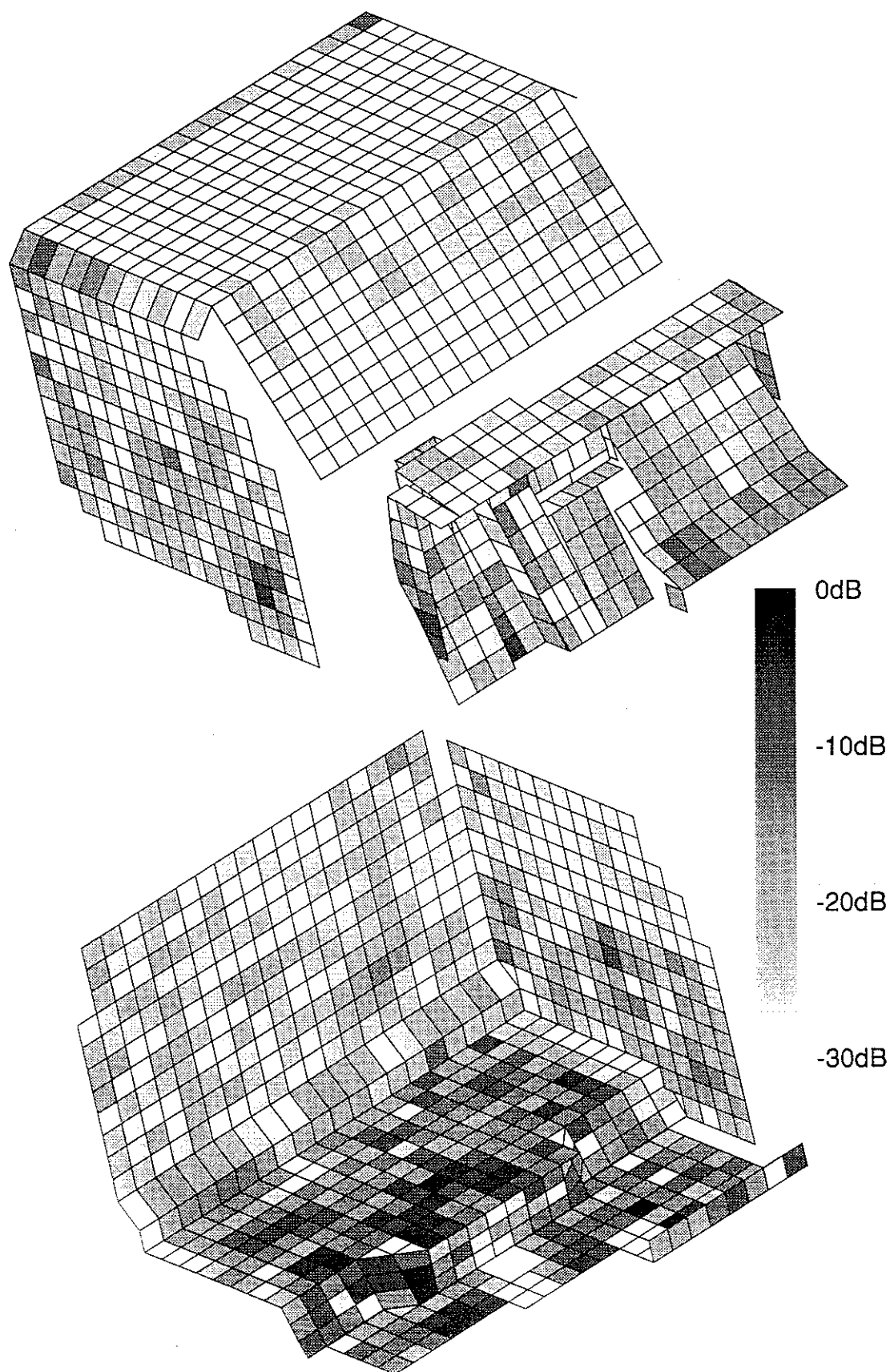
Figure 19 Distribution of Volume Velocity over the Interior Surface of the Vehicle Cab at 500Hz
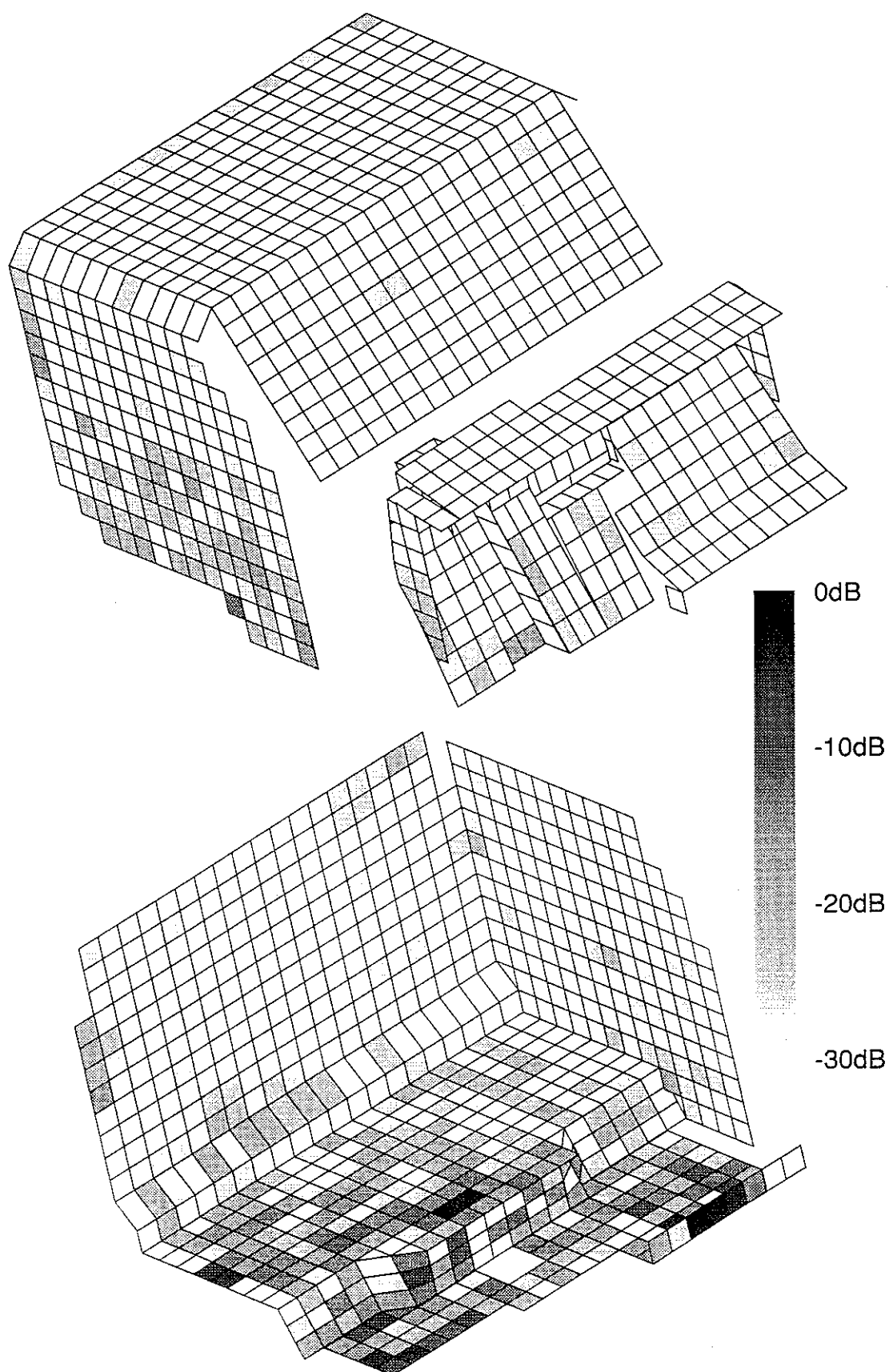
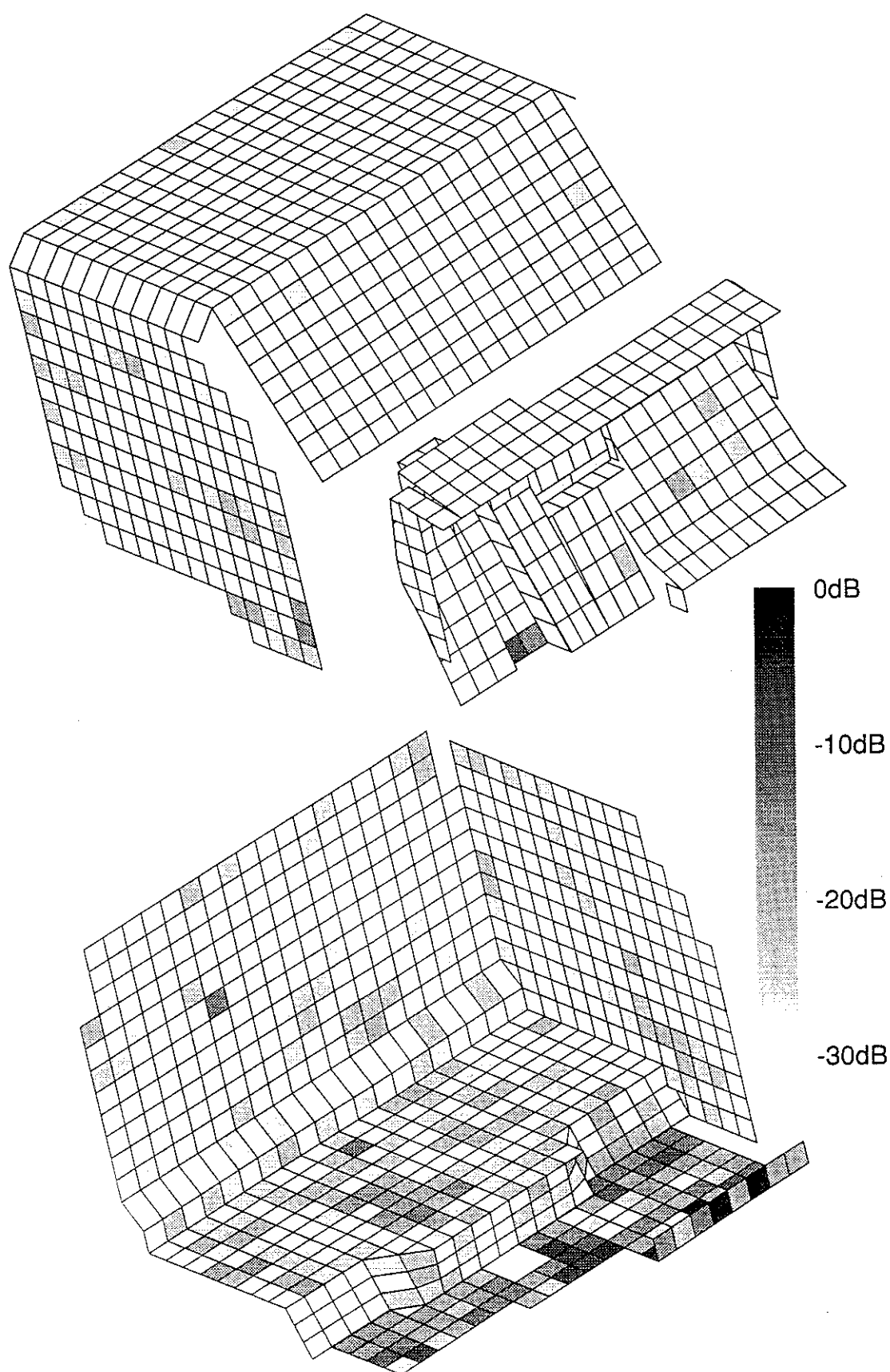*Figure 20 Distribution of Volume Velocity over the Interior Surface of the Vehicle Cab at 1000Hz*

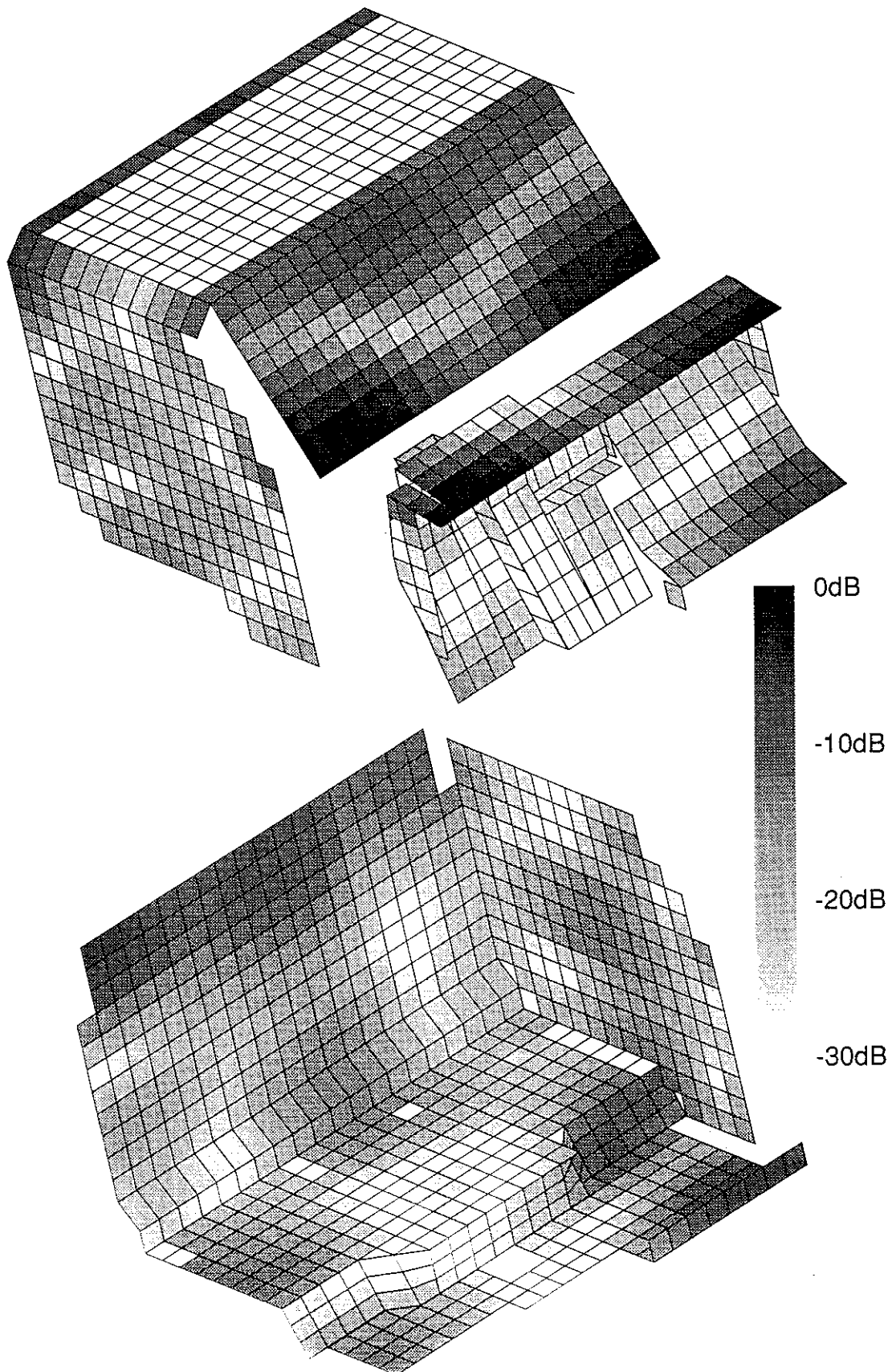*Figure 21 Distribution of Volume Velocity over the Interior Surface of the Vehicle Cab at 1600Hz*

Figure 22 Distribution ... ... interior Surface of the Vehicle Cab at

Figure 23   ....   Surface of the Vehicle Cab at

Figure 24 Distribution of Area Function over the Interior Surface of the Vehicle Cab at

Figure ⁣⁣ *Surface of the Vehicle Cab at*

Figure 26 Distribution of Pressure Contribution over the Interior Surface of the Vehicle Cab at 400Hz

Figure 27 Distribution of Pressure Contribution over the Interior Surface of the Vehicle Cab at 600Hz

Figure 28 Distribution of Pressure Contribution over the Interior Surface of the Vehicle Cab at 1000Hz
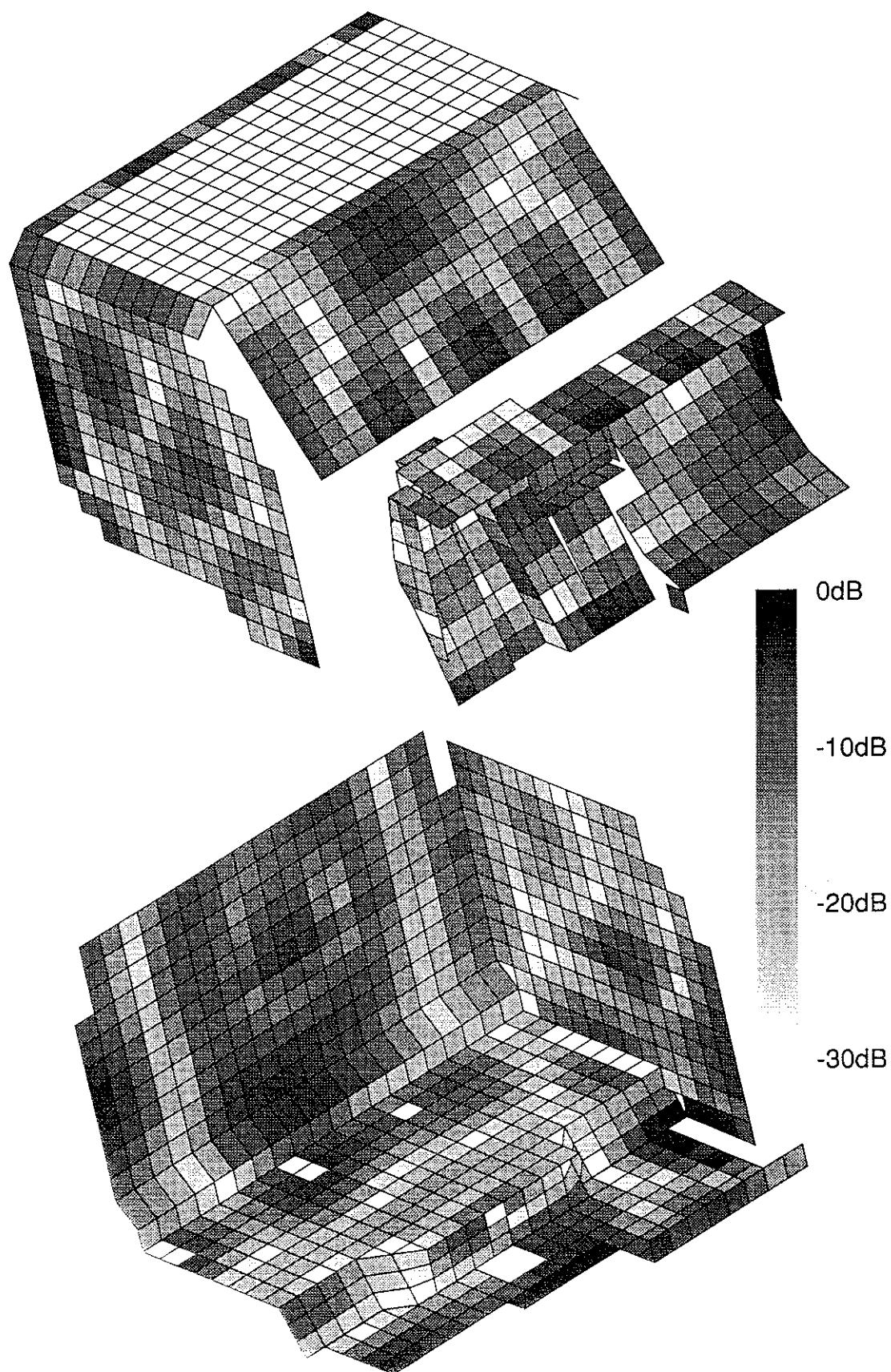
Figure 29 Distribution of Pressure Contribution over the Interior Surface of the Vehicle Cab at 1600Hz
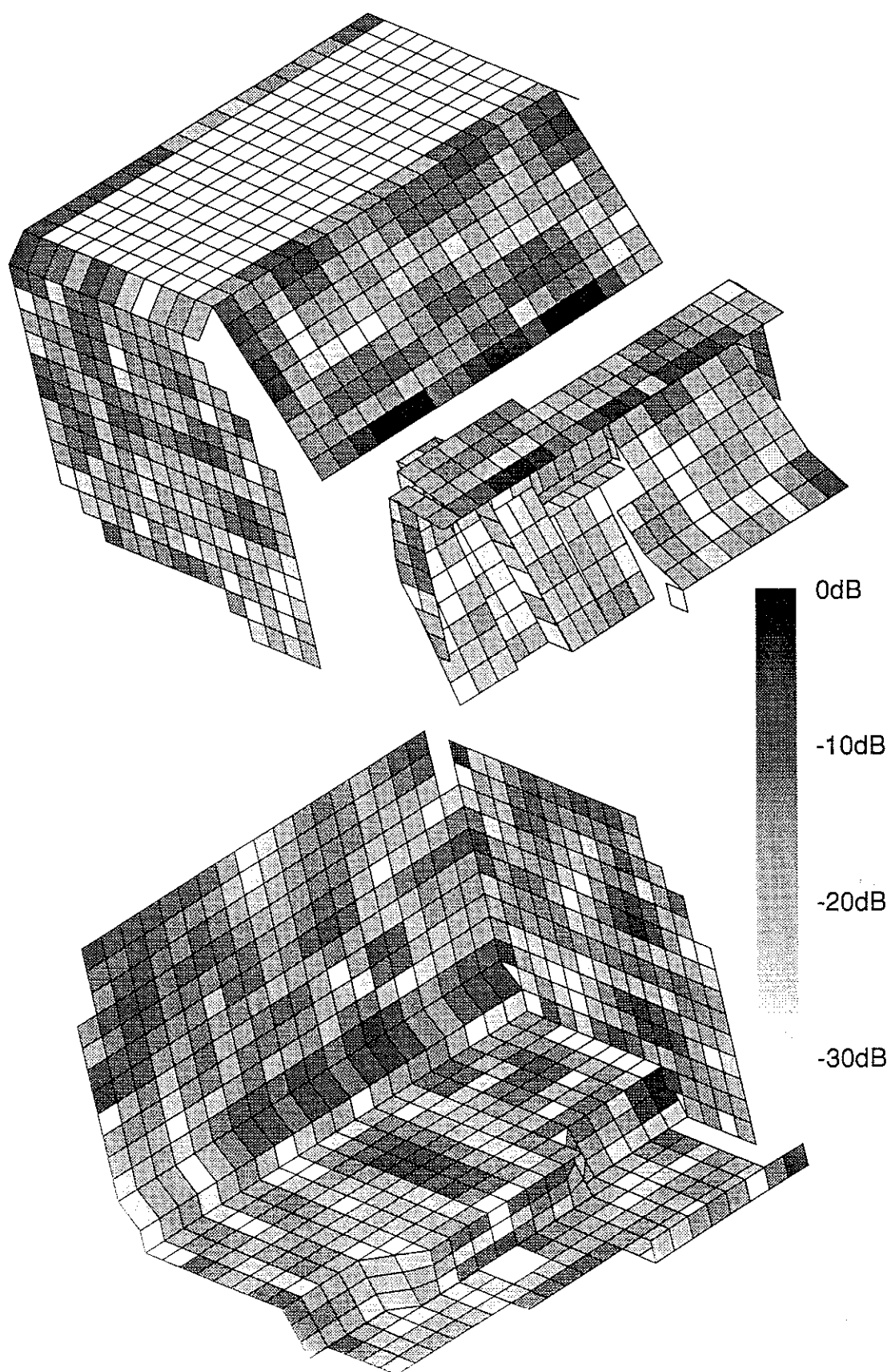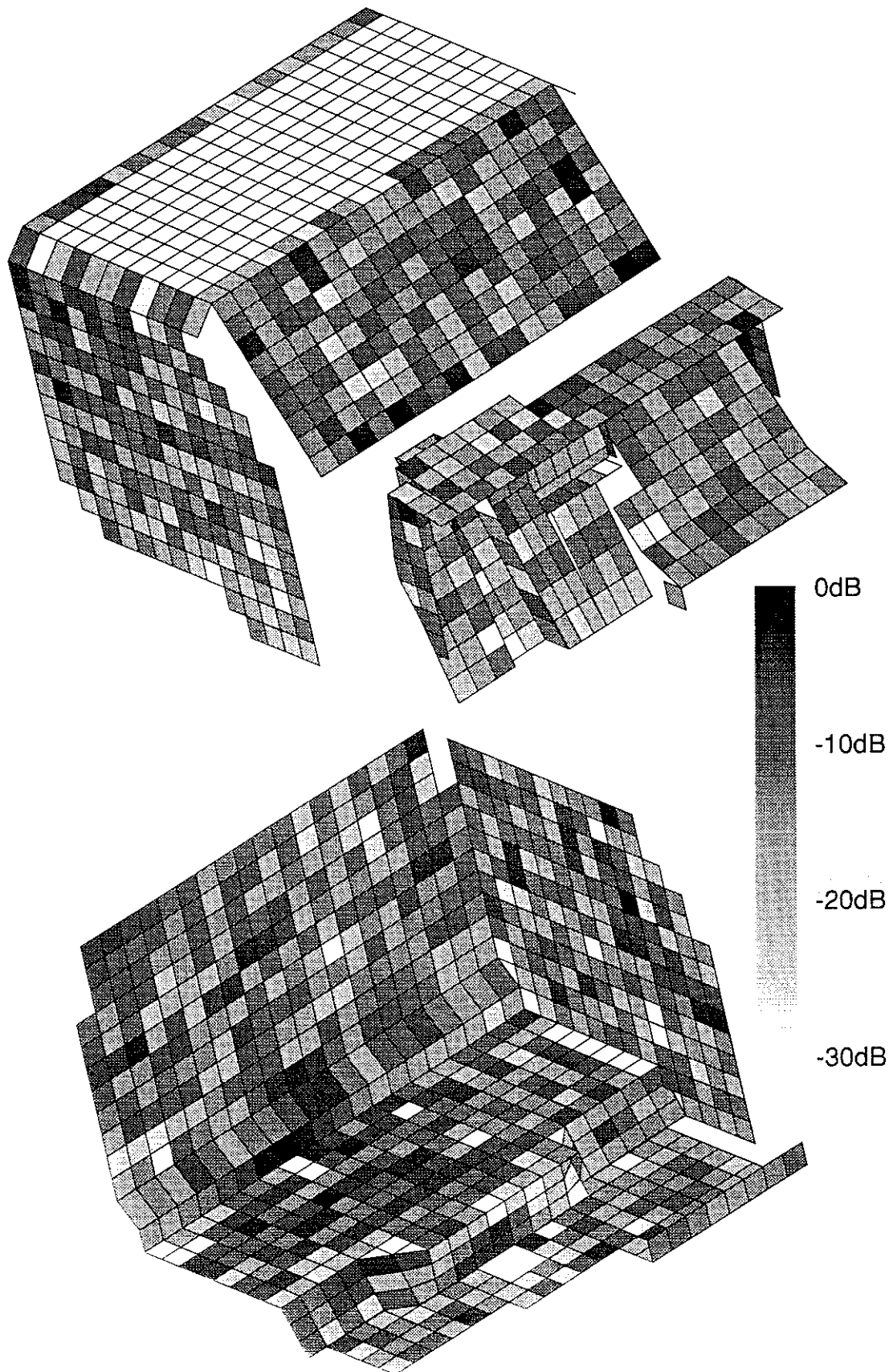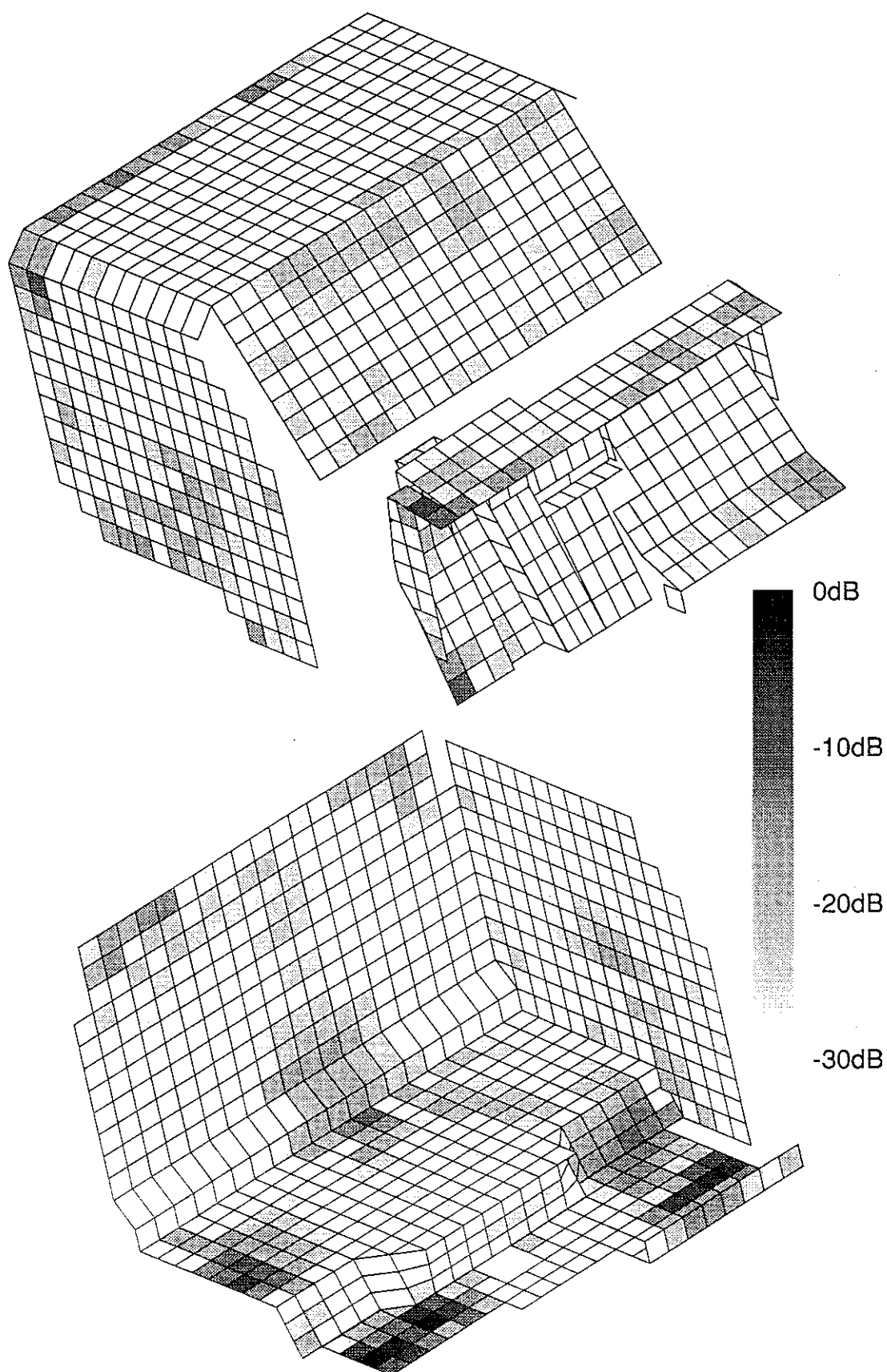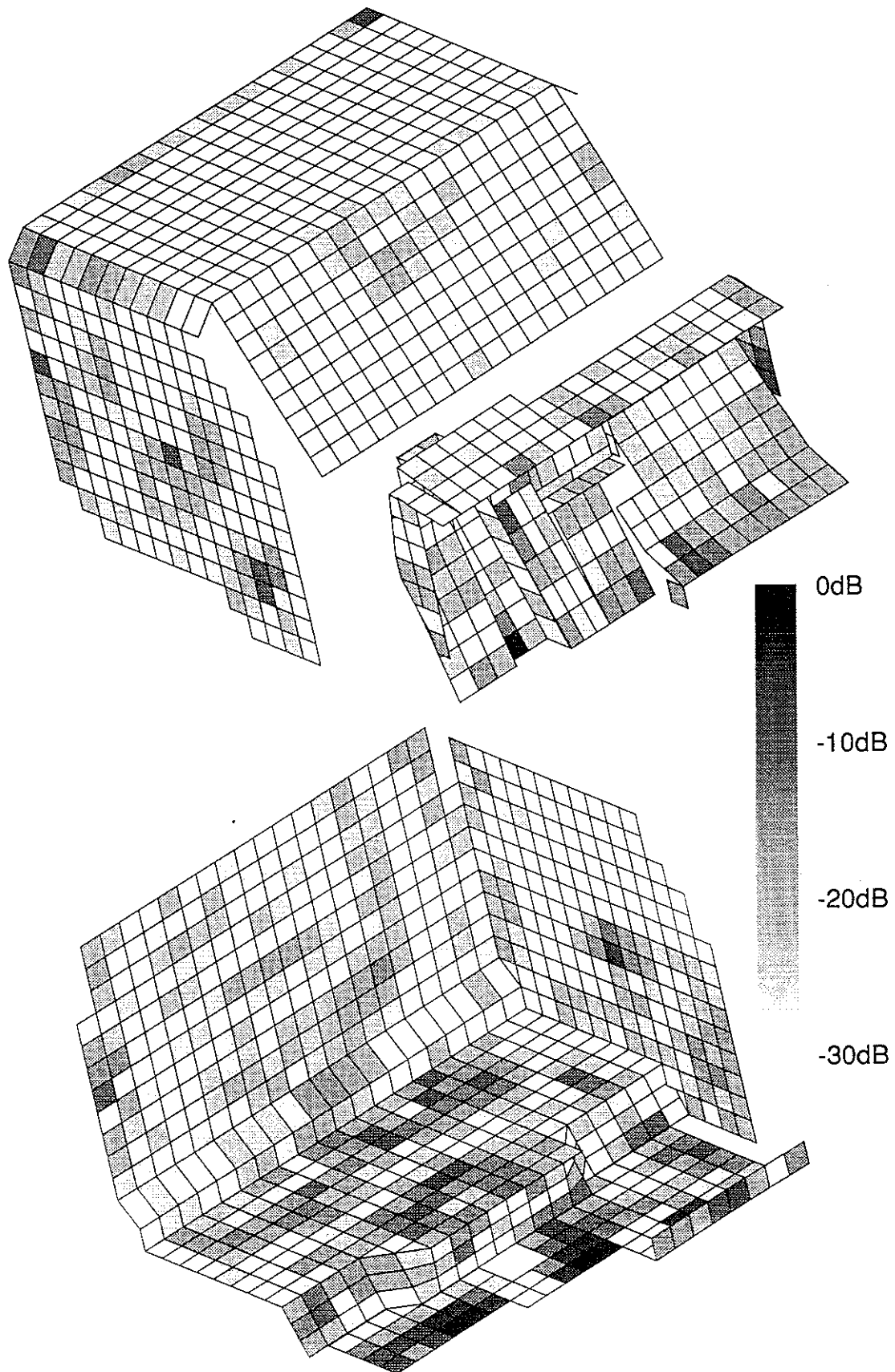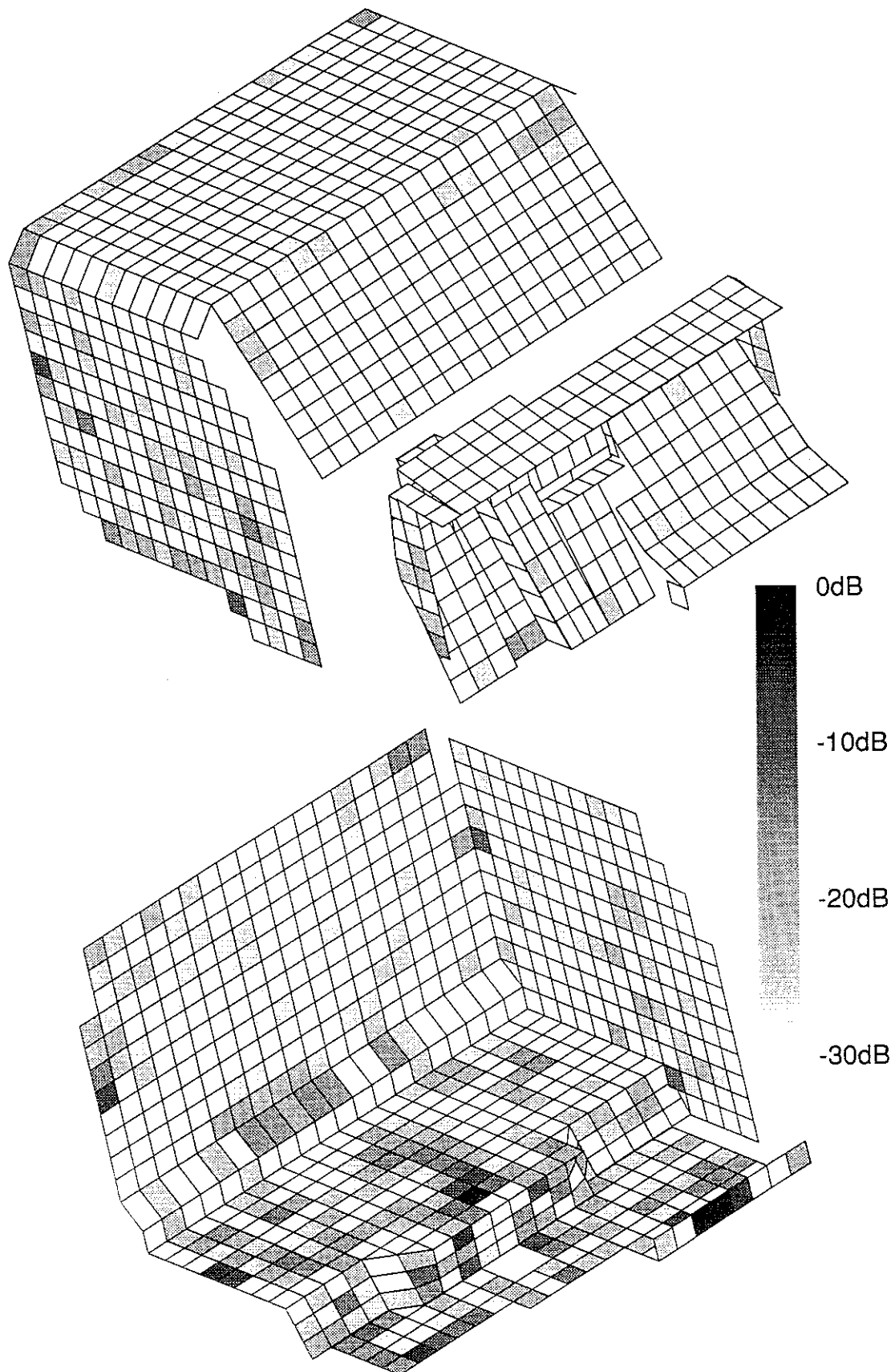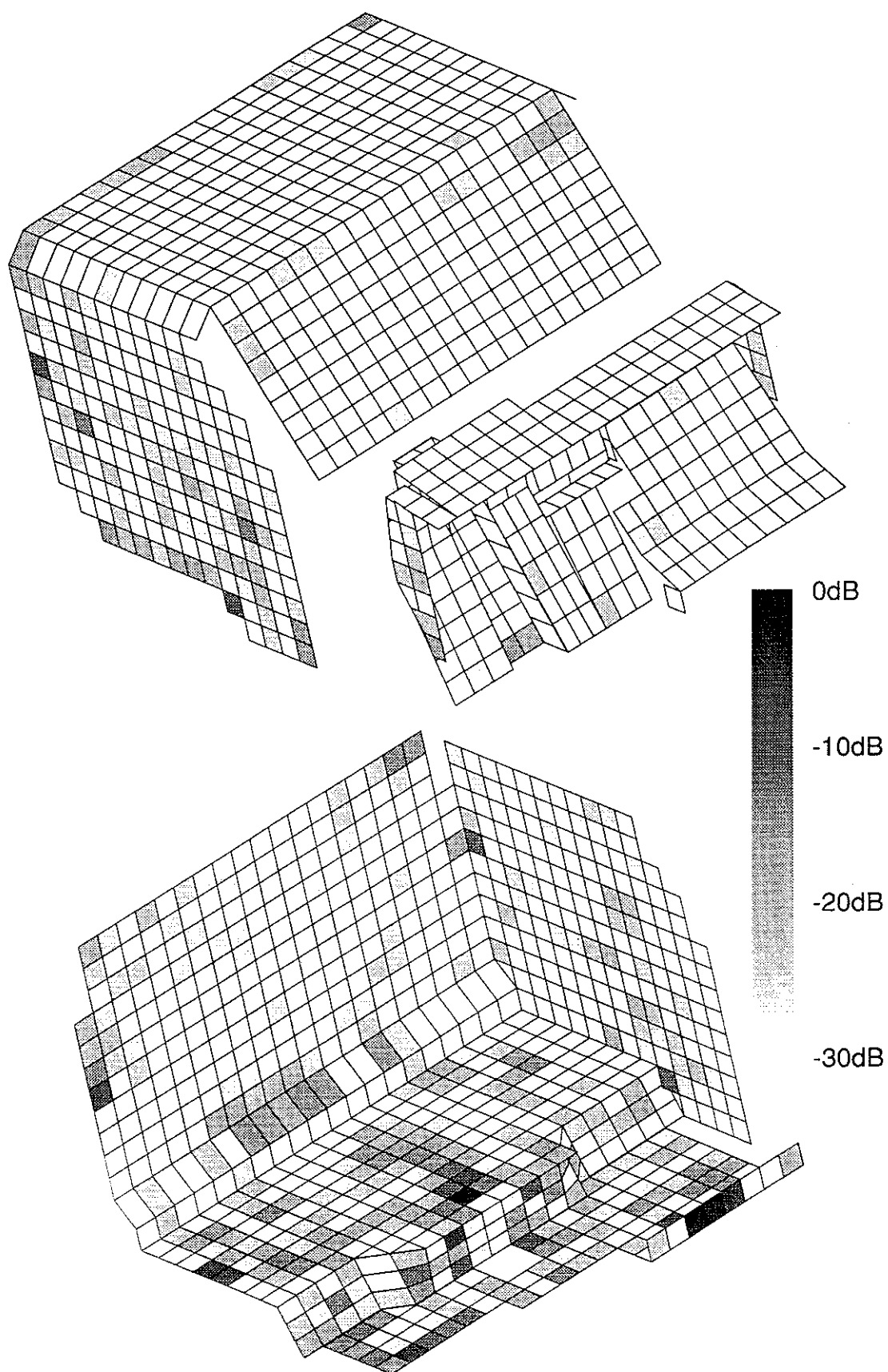
Figure 30 Calibration Curve for Transducer with Skirt Fitted

4.2 Validation Results.

Figure 31 shows a comparison between the directly measured pressure level (relative to the reference microphone) and that calculated from the 3208 measurements using equation (3). For clarity, figure 32 shows the same results but with the resolution reduced to 10Hz (200 points). The reduction in resolution was achieved by frequency smoothing the data using an eight point Hanning window before resampling – thus preserving much of the important detail (note: this is not the same as measuring 200 point transfer functions).

Figure 33 shows the result of ignoring the phase information in equation (3); the summation in this case takes the form:

$$S_{pr}(\omega) = |V_{ref}(\omega)|^2 \sum_{i}^{N} \left| \frac{V_i(\omega)}{V_{ref}(\omega)} A_i H_{ir} \right|^2 .$$

Figure 31 Comparison between Directly Measured Pressure Level and that Calculated from 3208 Measurements – 1.25Hz Resolution

Figure 32 Comparison between Directly Measured Pressure Level and that Calculated from 3208 Measurements – Resolution Reduced to 10Hz for Clarity
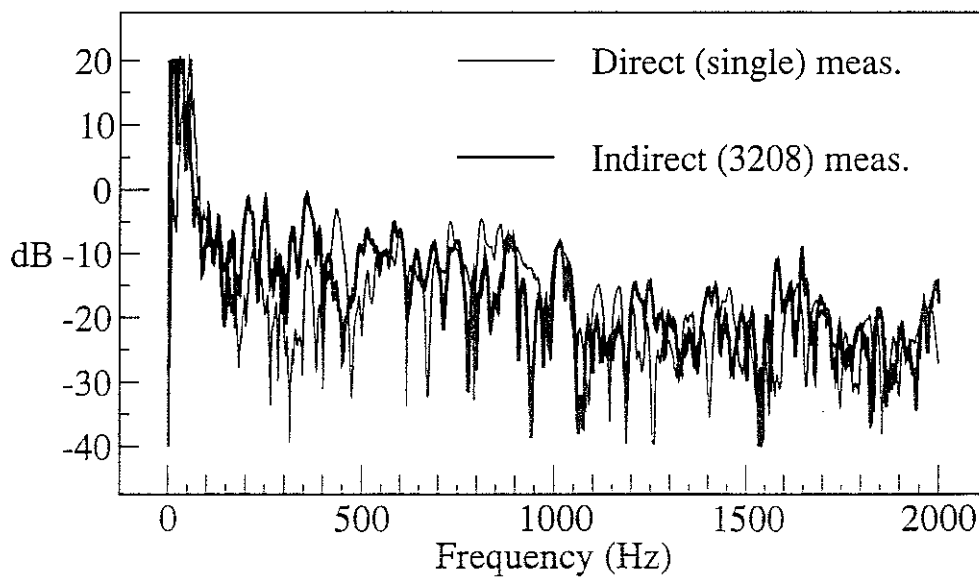

Figure 33 Comparison between Directly Measured Pressure Level and that Calculated from 3208 Measurements – Phase Ignored in Summation (10Hz Resolution)

4.3 Discussion of Results.

The result shown in figures 31 and 32 show that, on the whole, the validation test was successful. Although there is significant difference between the directly and indirectly measured results at some frequencies, the individual spectral peaks agree fairly well, and the overall character of the spectrum agrees well for frequencies above about 500Hz. The poor result at low frequencies can be explained by considering the ingress of reverberant sound into the transducer. Figure 26 shows that most of the sound at low frequencies is radiated by a small number of

elements. The contribution of the reverberant sound to the output of the transducer when measuring each of the rest of the elements is small but there are many of them, and when the large number of small contributions are summed, they give rise to a higher apparent sound level than the 'real' contribution from the radiating elements. Figure 34 shows the result of ignoring any individual element that contributes less than one tenth (-20dB) of the level of the highest contributing element. It can be seen that the result at low frequencies is now much better, but at the expense of accuracy at higher frequencies where the contribution is spread more evenly over more elements. The ingress of sound into the transducer is not expected to be a problem when measurements are confined to smaller areas; in the evaluation of a door trim for example.
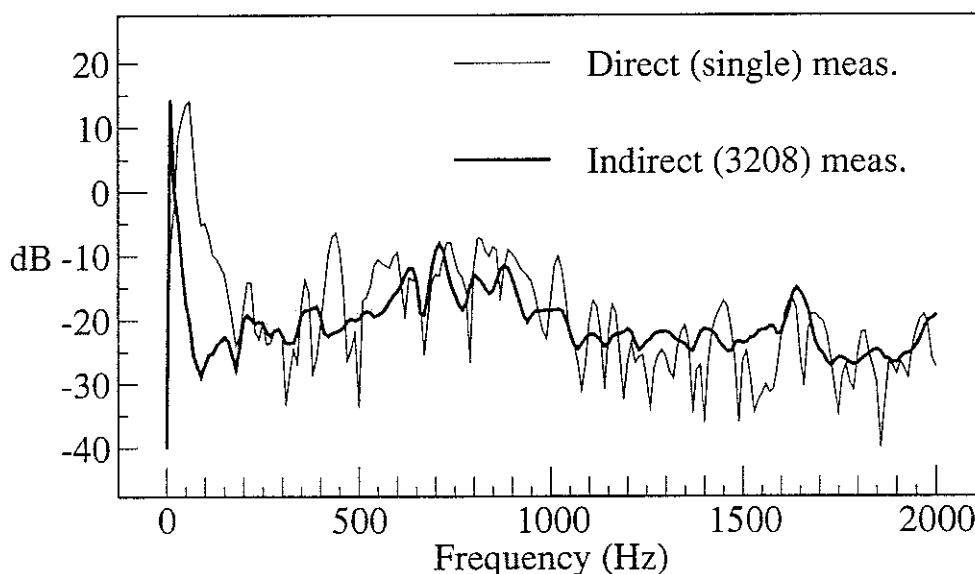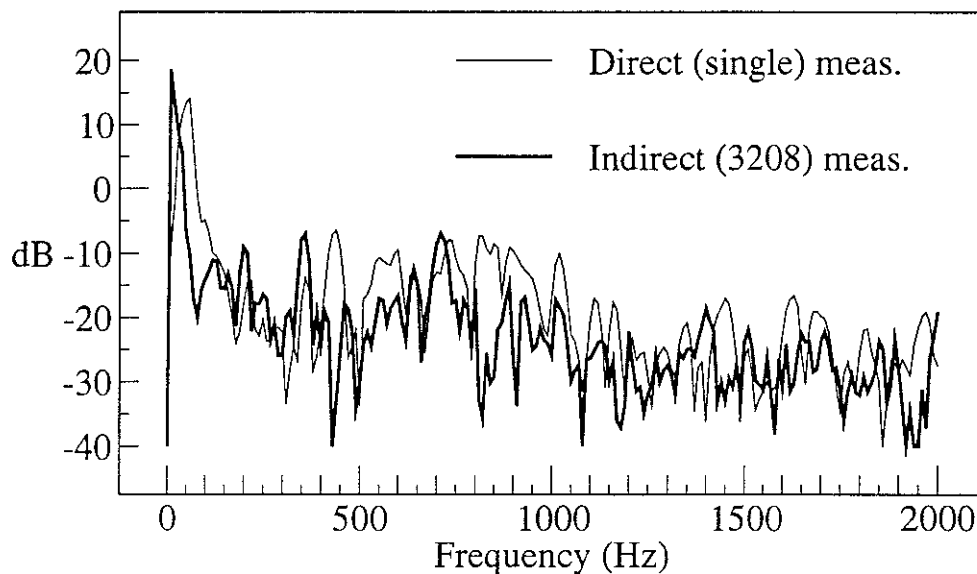

Figure 34 Comparison between Directly Measured Pressure Level and that Calculated from 3208 Measurements – Contributions below -20dB Ignored (10Hz Resolution)

Another possible source of error is the contribution to the noise level by sources that were not measured. Although great care was taken to seal all apertures, it is probable that some evaded detection; these sources would contribute to the direct measurement but not to the indirect. Initial measurements showed that the elements of the roof did not appear to contribute significantly and were thus assumed to behave passively; the roof does however have a large surface area and it is possible that the total contribution may be significant.

The validation test took place out-of-doors during a season with variable whether, and the 3208 transfer function measurements were necessarily spread over a long time period; it is probable that temperature and humidity variations are responsible for some of the differences between the results. Three repeats of the direct measurement throughout the period of the test showed little variation but more checks would have been desirable as subtle variations – particularly in phase – can multiply when combining such a large number of measurements.

It has been shown in section 1 that use of an accelerometer to estimate volume velocity gives rise to spatial aliasing of the vibration field and subsequent over-estimation of the contribution to the radiated field. Accelerometers were used in approximately 300 of the 1602 volume velocity measurements, including some of the floor elements which were found to contribute strongly. It

is likely that if it had been possible to use the integrating transducer for these elements that an improvement in results would be apparent. Further development of the transducer to include a long flexible tube to mount the anechoic termination away from the microphone section may help to resolve this problem.

A fairly respectable result is shown in figure 33 when the summation is carried out without regard for the phase information in the measurements. This result is encouraging as it shows that the experiment could have been carried out without the phase reference signals – only the autospectra would then need to be stored giving rise to a 50% reduction in data. This result also indicates that similar results could be achieved when more than one input source is active. In this case, the full set of $N \times N$ cross spectra are required (equation (2)), but if phase can be ignored, this would reduce to N measurements. Some loss of detail is apparent in figure 33 however, so the phase information is essential if narrow band detail is required.

5 Conclusions

A technique for evaluating the contribution of vibrating surfaces to vehicle interior noise has been described, and a suitable transducer for measuring the necessary elemental volume velocities has been developed. The technique has been evaluated on a full-sized vehicle and has proved successful for estimating the contribution of the various vibrating surfaces with the vehicle to the interior noise level.

6 References

[1] K R Holland and F J Fahy, "A Simple Transducer of Surface Vibrational Volume Velocity", in Proceedings of the Institute of Acoustics, 15(3), Acoustics 93, 1993.

[2] K R Holland and F J Fahy, "A Simple Vibrational Volume Velocity Transducer", in Proceedings of Inter-noise 93, Leuven, 1993.

[3] J-P Dalmont, J Kergomard et X Meynial, "Réalisation d'une Terminaison Anéchoïque pour un Tuyau Sonore aux Basses Fréquences", C. R. Acad. Sci. Paris, t. 309 Serie II, p. 453-458, 1989.

[4] A Craggs, "A Finite Element Model for Rigid Porous Absorbing Materials", J. Sound.Vib. 61, 1978

[5] P M Morse & K U Ingard, "Theoretical Acoustics", McGraw-Hill Book Co. Inc., New York, 1968.

[6] C D Smith & T L Parrott, "Comparison of Three Methods for Measuring Acoustic Properties of Bulk Materials", J Acoust. Soc. Am., 74(5), November 1983.

[7] F. J. Fahy, "Rapid Method for the Measurement of Sample Acoustic Impedance in a Standing Wave Tube", Letter to Editor, J. Sound Vib., 97(1) p168, 1984.